PHYSICAL REVIEW C **93**, 054618 (2016)

Nuclear spin of odd-odd α emitters based on the behavior of α-particle preformation probability

M. Ismail,[1] A. Adel,[1,2,*] and M. M. Botros[1]

[1]*Physics Department, Faculty of Science, Cairo University, Giza, Egypt*

[2]*Physics Department, College of Science, Majmaah University, Zulfi, Kingdom of Saudi Arabia*

(Received 1 November 2015; revised manuscript received 3 April 2016; published 23 May 2016)

The preformation probabilities of an α cluster inside radioactive parent nuclei for both odd-even and odd-odd nuclei are investigated. The calculations cover the isotopic chains from Ir to Ac in the mass regions $166 \leqslant A \leqslant 215$ and $77 \leqslant Z \leqslant 89$. The calculations are employed in the framework of the density-dependent cluster model. A realistic density-dependent nucleon-nucleon (NN) interaction with a finite-range exchange part is used to calculate the microscopic α-nucleus potential in the well-established double-folding model. The main effect of antisymmetrization under exchange of nucleons between the α and daughter nuclei has been included in the folding model through the finite-range exchange part of the NN interaction. The calculated potential is then implemented to find both the assault frequency and the penetration probability of the α particle by means of the Wentzel-Kramers-Brillouin approximation in combination with the Bohr-Sommerfeld quantization condition. The correlation of the α-particle preformation probability and the neutron and proton level sequences of the parent nucleus as obtained in our previous work is extended to odd-even and odd-odd nuclei to determine the nuclear spin and parities. Two spin coupling rules are used, namely, strong and weak rules to determine the nuclear spin for odd-odd isotopes. This work can be a useful reference for theoretical calculation of undetermined nuclear spin of odd-odd nuclei in the future.

DOI: 10.1103/PhysRevC.93.054618

I. INTRODUCTION

In recent years, the investigation of the α decay of radioactive nuclei has become a very interesting and popular research topic in nuclear physics, as it provides a powerful and useful tool for probing nuclear structure [1–5]. It can provide reliable information on ground-state lifetime, nuclear charge radius, nuclear incompressibility, nuclear spin, parity, and the collective excitations of the involved nuclei [6–11]. Moreover, the α decay plays a key role in the recent exploration of the island of stability of the newly synthesized superheavy nuclei [12–15].

The α-decay process is treated conventionally as the tunneling process of the preformed α particle through an interaction potential barrier between the cluster and core nucleus [16]. The α-decay half-life of the radioactive nucleus is completely determined by the decay width. In the cluster model, the decay width is well described as a product of three model-dependent quantities, namely, the barrier penetration probability which can be obtained in terms of the well-known Wentzel-Kramers-Brillouin (WKB) semiclassical approximation, the assault frequency, and the preformation probability of the emitted clusters inside the decaying nucleus.

An interesting aspect in α decay is how to estimate the α preformation probability, which gives the probability that the α particle exists as a recognizable entity inside the nucleus before its emission [17]. The determination of the exact value of the preformation factor is essential for improving the accuracy of theoretical calculations. It would help in estimating the half-lives of the superheavy elements which affect their survival probability against different decay channels. On the other hand, this preformation factor is considered to carry most of the valuable information about nuclear structure, especially about the dynamic states of nucleons around the nuclear surface[18]. It is expected to reflect the influences of the different nuclear structure properties of the parent and its decay components, such as their isospin asymmetry[19], shell and pairing effects [20], and their deformations [21–23]. It was revealed in our recent studies [24–26] that the behavior of the preformation factor is associated with the neutron and proton level sequences of the parent nucleus, and can be used to predict the nuclear spin for both even-even and even-odd nuclei. Moreover, it was pointed out that the existence of unpaired nucleons in the open shells of the parent nucleus influences the preformation mechanism [27]. The α-cluster preformation probability inside the nuclei that have unpaired nucleons is less than it would be in the neighboring nuclei of the same shell and subshell closures but have no unpaired nucleons [27].

In principle, the preformation factor can be calculated from the overlap between the actual wave function of the parent nucleus and the wave function of the decaying state describing the α particle coupled to the residual daughter nucleus [28,29]. In these calculations, the wave function is necessary, and it is not easy to include very large basis and massive configuration mixing to access the actual wave function, which becomes even more sophisticated when more nucleons relevant to the preformation are considered. Several factors may affect the calculated values of the α-preformation probability from different theoretical approaches such that the deformation of the involved nuclei, the isospin asymmetry, and the angular momentum transfer in case of involved nuclei include odd nucleon numbers. It should be noted that the extracted α-preformation factors are different for various models; that is, they are model-dependent factors [30–33]. More strikingly, the varying trend of the preformation factor, such as for an isotopic chain, is model independent [34].

*ahmedadel@sci.cu.edu.eg, aa.ahmed@mu.edu.sa

 ©2016 American Physical Society

In a previous work [24–26], we studied the correlation between α-particle preformation probability, S_α, and the energy levels of parent nuclei for a wide range of even-even and even-odd nuclei. We also clarified how to predict unknown or confirm the doubted nuclear spins and parities for these kind of nuclei.

The aim of the present paper is to clarify the rules used to determine the total nuclear spin and parities for α emitters with atomic number $77 \leqslant Z \leqslant 89$ for both odd-even and odd-odd nuclei based on the behavior of α-particle preformation probability. In odd-A and odd-odd nuclei, the ground-state spin-parities of parent and daughter nuclei are generally different, leading to the hindrance of the additional centrifugal barrier. Therefore, the transitions between ground states are hindered ones. Theoretically, the hindered α transition is an effective tool to study the properties of α emitters because it is closely related to the internal structure of nuclei.

The outline of the paper is as follows. In Sec. II a description of the microscopic nuclear and Coulomb potentials between the α and daughter nuclei is given. The methods for determining the decay width, the penetration probability, the assault frequency, and the preformation probability are also presented. In Sec. III, the calculated results are discussed. Finally, Sec. IV gives a brief conclusion.

II. THEORETICAL FRAMEWORK

In the performed cluster models, the α particle is considered to be formed with a definite probability as an individual cluster inside the parent nucleus at the preliminary stage. Once formed, it will try to emit, leaving the daughter nucleus behind. The α-decay partial half-lifetime, $T_{1/2}$, of the parent nucleus is given in terms of the α-decay width, Γ, as

$$T_{1/2} = \frac{\hbar \ln 2}{\Gamma}. \tag{1}$$

The absolute α decay width is mainly determined by the barrier penetration probability (P_α), the assault frequency (ν), and the preformation probability (S_α), $\Gamma = \hbar\, S_\alpha\, \nu\, P_\alpha$. The barrier penetration probability, P_α, could be calculated as the barrier transmission coefficient of the well-known Wentzel-Kramers-Brillouin (WKB) approximation, which works well at energies well below the barrier:

$$P_\alpha = \exp\left(-2\int_{R_2}^{R_3} dr \sqrt{\frac{2\,\mu}{\hbar^2}\,|V_T(r) - Q_\alpha|}\right). \tag{2}$$

Here μ is the reduced mass of the cluster-core system and Q_α is the Q value of the α decay. $R_i (i = 1,2,3)$ are the three turning points for the α-daughter potential barrier, where $V_T(r)|_{r=R_i} = Q_\alpha$.

The assault frequency of the α particle, ν, can be expressed as the inverse of the time required to traverse the distance back and forth between the first two turning points, R_1 and R_2, as [35]

$$\nu = T^{-1} = \frac{\hbar}{2\,\mu}\left[\int_{R_1}^{R_2} \frac{dr}{\sqrt{\frac{2\,\mu}{\hbar^2}\,|V_T(r) - Q_\alpha|}}\right]^{-1}. \tag{3}$$

The total interaction potential of the α-core system comprises the nuclear and the Coulomb potentials plus the centrifugal part, and is given by [5,36]

$$V_{\rm T}(R) = \lambda\, V_N(R) + V_C(R) + \frac{\hbar^2}{2\,\mu}\frac{\left(\ell + \frac{1}{2}\right)^2}{R^2}, \tag{4}$$

where R is the separation distance between the mass center of the α particle and the mass center of the core. The latter term in Eq. (4) represents the Langer modified centrifugal potential, and ℓ is the angular momentum carried by the α particle. The value of angular momentum ℓ, which is used for the calculation of the centrifugal term, is arranged in column five of Table I. These are the minimum values of possible angular momenta; the α particle can transfer any value of the angular momentum according to the following spin-parity selection rule:

$$|J_i - J_f| \leqslant \ell \leqslant |J_i + J_f| \quad \text{and} \quad \frac{\pi_f}{\pi_i} = (-1)^\ell, \tag{5}$$

where J_i, π_i and J_f, π_f are the spin and parity of parent and daughter nuclei, respectively.

The renormalization factor λ, introduced to the nuclear part of the folding potential based on the M3Y interaction, is not an adjustable parameter, but it is determined separately for each decay by applying the Bohr-Sommerfeld quantization condition

$$\int_{R_1}^{R_2} dr \sqrt{\frac{2\,\mu}{\hbar^2}\,|V_T(r) - Q_i|} = (G - \ell + 1)\frac{\pi}{2}, \tag{6}$$

where the global quantum number $G = 20$ ($N > 126$) and $G = 18$ ($82 < N \leqslant 126$) [36]. In Ref. [35], the half-lives are found to be sensitive to the implementation of this condition in the WKB approach, which fixes the depth of the double-folding nuclear potential λ.

The nuclear part of the potential, $V_N(R)$, consists of two terms: the direct, $V_D(R)$, and the exchange, $V_{\rm Ex}(R)$, terms. The direct part of the nuclear interaction potential between two colliding nuclei and the equation describing the Coulomb interaction have similar forms involving only diagonal elements of the density matrix [37,38]:

$$V_D(R) = \int d\vec{r}_1 \int d\vec{r}_2 \rho_\alpha(\vec{r}_1)\, \upsilon_D(\rho, E, s)\, \rho_d(\vec{r}_2), \tag{7}$$

where $s = |\vec{r}_2 - \vec{r}_1 + \vec{R}|$ is the relative distance between a constituent nucleon in the α particle and one in the daughter nucleus. E is the incident laboratory energy per nucleon. $\rho_\alpha(\vec{r}_1)$ and $\rho_d(\vec{r}_2)$ are, respectively, the density distributions of the α particle and the residual daughter nucleus as described in Ref. [36].

The exchange potential accounts for the knock-on exchange of nucleons between the interacting nuclei. The exchange term is, in general, nonlocal [39]

$$V_{\rm Ex}(E,R) = \int d\vec{r}_1 \int d\vec{r}_2 \rho_\alpha(\vec{r}_1, \vec{r}_1 + \vec{s})\, \rho_d(\vec{r}_2, \vec{r}_2 - \vec{s}) \times \upsilon_{\rm Ex}(\rho, E, s) \exp\left[\frac{i\vec{k}(R)\cdot\vec{s}}{M}\right]. \tag{8}$$

TABLE I. The preformation probability, S_α, and the α-decay half-lives, $T_{1/2}^{\rm calc}$, calculated without S_α for Ir, Au, Tl, Bi, At, Fr, and Ac isotopes using the CDM3Y1-Paris NN interaction. Experimental Q values, α-decay half-lives, and spins and parities are taken from Ref. [48]. Uncertain spin and/or parity assignments are in parentheses. The sign * means the spin and/or parity assignments as well as the angular momentum of transition are modified according to the behavior of S_α and their modified values are in square brackets beside the values used in our calculations. The sign † means the tabulated spin is confirmed by the behavior of S_α.

Reaction	$Q_\alpha^{\rm expt}$ (MeV)	J_i^π	J_f^π	$\ell_{\rm min}$	$T_{1/2}^{\rm expt}$ (s)	$T_{1/2}^{\rm calc}$ (s)	S_α
^{166}Ir → ^{162}Re + α	6.722 ± 0.006	$(2^-)^\dagger$	(2^-)	0	$(1.13 \pm 0.24) \times 10^{-2}$	$8.02^{+0.40}_{-0.38} \times 10^{-4}$	0.071 ± 0.015
^{167}Ir → ^{163}Re + α	6.505 ± 0.003	$1/2^+$	$1/2^+$	0	$(7.33 \pm 0.42) \times 10^{-2}$	$4.62^{+0.12}_{-0.12} \times 10^{-3}$	0.063 ± 0.004
^{169}Ir → ^{165}Re + α	6.141 ± 0.004	$(1/2^+)^\dagger$	$(1/2^+)$	0	$(7.84 \pm 0.09) \times 10^{-1}$	$1.07^{+0.04}_{-0.04} \times 10^{-1}$	0.137 ± 0.005
^{171}Ir → ^{167}Re + α	6.001 ± 0.015	$(11/2^-)^\dagger$	$(9/2^-)$	2	$(3.10 \pm 0.30) \times 10^{0}$	$7.2^{+1.1}_{-1.0} \times 10^{-1}$	0.233 ± 0.040
^{172}Ir → ^{168}Re + α	5.991 ± 0.010	$(3^+)^\dagger$	(7^+)	4	$(2.20 \pm 0.15) \times 10^{2}$	$3.45^{+0.35}_{-0.32} \times 10^{0}$	0.016 ± 0.002
^{173}Ir → ^{169}Re + α	5.716 ± 0.010	$(3/2^+),(5/2^+)^\dagger$	$(9/2^-)$	3	$(1.29 \pm 0.11) \times 10^{2}$	$2.20^{+0.24}_{-0.22} \times 10^{1}$	0.172 ± 0.023
^{174}Ir → ^{170}Re + α	5.624 ± 0.010	$(3^+)^\dagger$	(5^+)	2	$(1.58 \pm 0.12) \times 10^{3}$	$2.90^{+0.33}_{-0.29} \times 10^{1}$	0.018 ± 0.002
^{175}Ir → ^{171}Re + α	5.430 ± 0.030	$(5/2^-)^\dagger$	$(9/2^-)$	2	$(1.06 \pm 0.24) \times 10^{3}$	$2.33^{+0.94}_{-0.66} \times 10^{2}$	0.233 ± 0.091
^{177}Ir → ^{173}Re + α	5.080 ± 0.030	$5/2^-$	$(5/2^-)$	0	$(5.00 \pm 0.33) \times 10^{4}$	$7.0^{+3.2}_{-2.2} \times 10^{3}$	0.150 ± 0.054
^{170}Au → ^{166}Ir + α	7.177 ± 0.015	$(2^-)^\dagger$	(2^-)	0	$(2.60 \pm 0.46) \times 10^{-3}$	$1.56^{+0.18}_{-0.16} \times 10^{-4}$	0.060 ± 0.013
^{173}Au → ^{169}Ir + α	6.836 ± 0.005	$(1/2^+)^\dagger$	$(1/2^+)$	0	$(2.66 \pm 0.11) \times 10^{-2}$	$1.96^{+0.08}_{-0.08} \times 10^{-3}$	0.074 ± 0.004
^{177}Au → ^{173}Ir + α	6.298 ± 0.004	$(1/2^+)^\dagger,(3/2^+)$	$(3/2^+,5/2^+)$	2	$(3.65 \pm 0.08) \times 10^{0}$	$3.24^{+0.12}_{-0.12} \times 10^{-1}$	0.089 ± 0.004
^{179}Au → ^{175}Ir + α	5.981 ± 0.005	$(1/2^+)^\dagger,(3/2^+)$	$(5/2^-)$	3	$(3.23 \pm 0.14) \times 10^{1}$	$1.18^{+0.06}_{-0.06} \times 10^{1}$	0.365 ± 0.024
^{181}Au → ^{177}Ir + α	5.751 ± 0.003	$(3/2^-)[5/2^{-*}]$	$5/2^-$	2[0*]	$(5.07 \pm 0.52) \times 10^{2}$	$6.07^{+0.20}_{-0.19} \times 10^{1}$	0.120 ± 0.013
^{183}Au → ^{179}Ir + α	5.465 ± 0.003	$(5/2)^{-\dagger}$	$(5/2)^-$	0	$(7.78 \pm 0.18) \times 10^{3}$	$6.84^{+0.24}_{-0.23} \times 10^{2}$	0.088 ± 0.004
^{184}Au → ^{180}Ir + α	5.234 ± 0.005	5^+	$(4,5)$	2	$(1.29 \pm 0.06) \times 10^{5}$	$1.93^{+0.12}_{-0.11} \times 10^{4}$	0.150 ± 0.011
^{185}Au → ^{181}Ir + α	5.180 ± 0.005	$5/2^-$	$5/2^-$	0	$(9.81 \pm 0.14) \times 10^{4}$	$1.89^{+0.12}_{-0.11} \times 10^{4}$	0.193 ± 0.012
^{186}Au → ^{182}Ir + α	4.912 ± 0.014	3^-	3^+	1	$(8.03 \pm 0.38) \times 10^{7}$	$7.3^{+1.5}_{-1.2} \times 10^{5}$	0.009 ± 0.002
^{177}Tl → ^{173}Au + α	7.067 ± 0.007	$(1/2+)^\dagger$	$(1/2+)$	0	$(2.47 \pm 0.69) \times 10^{-2}$	$2.07^{+0.12}_{-0.11} \times 10^{-3}$	0.084 ± 0.024
^{179}Tl → ^{175}Au + α	6.710 ± 0.005	$(1/2+)^\dagger$	$(1/2+)$	0	$(2.30 \pm 0.40) \times 10^{-1}$	$3.56^{+0.15}_{-0.17} \times 10^{-2}$	0.154 ± 0.028
^{180}Tl → ^{176}Au + α	6.710 ± 0.005	$(4^-)^\dagger, (5^-)$	(5^-)	0[2*]	$(1.82 \pm 0.02) \times 10^{1}$	$3.44^{+0.14}_{-0.15} \times 10^{-2}$	0.002 ± 0.001
^{181}Tl → ^{177}Au + α	6.321 ± 0.006	$(1/2^+)^\dagger$	$(1/2^+,3/2^+)$	0	$(3.20 \pm 0.30) \times 10^{1}$	$1.06^{+0.06}_{-0.06} \times 10^{0}$	0.033 ± 0.004
^{184}Bi → ^{180}Tl + α	8.020 ± 0.005	$(3^+)^\dagger$	$(4^-,5^-)[2^{-*}]$	1	$(1.30 \pm 0.20) \times 10^{-2}$	$1.44^{+0.56}_{-0.40} \times 10^{-5}$	0.001 ± 0.001
^{185}Bi → ^{181}Tl + α	8.140 ± 0.080	$1/2^+$	$(1/2^+)$	0	$(5.80 \pm 0.40) \times 10^{-4}$	$5.2^{+3.5}_{-2.1} \times 10^{-6}$	0.010 ± 0.005
^{186}Bi → ^{182}Tl + α	7.757 ± 0.012	$(3^+)[2^{-*}]$	(7^+)	4[5*]	$(1.48 \pm 0.07) \times 10^{-2}$	$4.85^{+0.43}_{-0.39} \times 10^{-4}$	0.033 ± 0.003
^{187}Bi → ^{183}Tl + α	7.779 ± 0.004	$(9/2^-)^\dagger$	$(1/2^+)$	5	$(3.70 \pm 0.20) \times 10^{-2}$	$1.09^{+0.03}_{-0.03} \times 10^{-3}$	0.029 ± 0.002
^{188}Bi → ^{184}Tl + α	7.264 ± 0.005	$(10^-)[3^{+*}]$	$(7^+)[2^{-*}]$	3[1*]	$(2.65 \pm 0.15) \times 10^{-1}$	$7.51^{+0.36}_{-0.22} \times 10^{-3}$	0.029 ± 0.002
^{189}Bi → ^{185}Tl + α	7.268 ± 0.003	$(9/2^-)^\dagger$	$(1/2^+)$	5	$(1.35 \pm 0.02) \times 10^{0}$	$4.36^{+0.12}_{-0.09} \times 10^{-2}$	0.032 ± 0.001
^{190}Bi → ^{186}Tl + α	6.863 ± 0.004	$(3^+)[2^{-*}]$	(7^+)	4[5*]	$(7.00 \pm 0.11) \times 10^{0}$	$4.09^{+0.14}_{-0.15} \times 10^{-1}$	0.058 ± 0.002
^{191}Bi → ^{187}Tl + α	6.778 ± 0.003	$(9/2^-)^\dagger$	$(1/2^+)$	5	$(2.43 \pm 0.06) \times 10^{1}$	$2.27^{+0.06}_{-0.06} \times 10^{0}$	0.093 ± 0.003
^{192}Bi → ^{188}Tl + α	6.376 ± 0.005	$(3^+)^\dagger$	$(2^-)^\dagger$	1	$(2.88 \pm 0.08) \times 10^{2}$	$4.71^{+0.23}_{-0.22} \times 10^{0}$	0.016 ± 0.001
^{193}Bi → ^{189}Tl + α	6.304 ± 0.005	$(9/2^-)^\dagger$	$(1/2^+)$	5	$(1.82 \pm 0.09) \times 10^{3}$	$1.63^{+0.08}_{-0.08} \times 10^{2}$	0.090 ± 0.006
^{194}Bi → ^{190}Tl + α	5.918 ± 0.005	$(3^+)^\dagger$	$2^{(-)\dagger}$	1	$(2.07 \pm 0.07) \times 10^{4}$	$4.36^{+0.24}_{-0.23} \times 10^{2}$	0.021 ± 0.001
^{195}Bi → ^{191}Tl + α	5.832 ± 0.005	$(9/2^-)^\dagger$	$(1/2^+)$	5	$(6.10 \pm 0.13) \times 10^{5}$	$1.96^{+0.11}_{-0.10} \times 10^{4}$	0.032 ± 0.002
^{191}At → ^{187}Bi + α	7.822 ± 0.014	$(1/2^+)$	$(9/2^-)$	5	$(2.10 \pm 0.80) \times 10^{-3}$	$4.47^{+0.47}_{-0.42} \times 10^{-3}$	2.14 ± 0.84
^{193}At → ^{189}Bi + α	7.572 ± 0.007	$(1/2^+)$	$(9/2^-)$	5	$(2.90 \pm 0.50) \times 10^{-2}$	$2.57^{+0.14}_{-0.13} \times 10^{-2}$	0.89 ± 0.16
^{194}At → ^{190}Bi + α	7.463 ± 0.015	$(9^-,10^-)[7^{+*}]$	(3^+)	7[4*]	$(3.10 \pm 0.08) \times 10^{-1}$	$7.41^{+0.91}_{-0.81} \times 10^{-1}$	2.41 ± 0.28
^{195}At → ^{191}Bi + α	7.339 ± 0.005	$1/2^+$	$(9/2^-)$	5	$(3.28 \pm 0.20) \times 10^{-1}$	$1.42^{+0.06}_{-0.06} \times 10^{-1}$	0.435 ± 0.032
^{196}At → ^{192}Bi + α	7.198 ± 0.004	$(3^+)^\dagger$	(3^+)	0	$(4.08 \pm 0.07) \times 10^{-1}$	$2.09^{+0.07}_{-0.07} \times 10^{-2}$	0.051 ± 0.002
^{197}At → ^{193}Bi + α	7.100 ± 0.005	$(9/2^-)^\dagger$	$(9/2^-)$	0	$(4.04 \pm 0.06) \times 10^{-1}$	$4.47^{+0.19}_{-0.18} \times 10^{-2}$	0.111 ± 0.005
^{198}At → ^{194}Bi + α	6.890 ± 0.002	$(3^+)^\dagger$	(3^+)	0	$(4.22 \pm 0.44) \times 10^{0}$	$2.52^{+0.05}_{-0.05} \times 10^{-1}$	0.060 ± 0.006
^{199}At → ^{195}Bi + α	6.777 ± 0.001	$(9/2^-)^\dagger$	$(9/2^-)$	0	$(7.81 \pm 0.17) \times 10^{0}$	$6.51^{+0.07}_{-0.07} \times 10^{-1}$	0.083 ± 0.002
^{200}At → ^{196}Bi + α	6.596 ± 0.001	$(3^+)^\dagger$	(3^+)	0	$(8.27 \pm 0.19) \times 10^{1}$	$3.22^{+0.04}_{-0.04} \times 10^{0}$	0.039 ± 0.001
^{201}At → ^{197}Bi + α	6.473 ± 0.002	$(9/2^-)^\dagger$	$(9/2^-)$	0	$(1.20 \pm 0.02) \times 10^{2}$	$9.85^{+0.15}_{-0.15} \times 10^{0}$	0.082 ± 0.002
^{202}At → ^{198}Bi + α	6.354 ± 0.001	$(2^+),(3^+)^\dagger$	$(2^+,3^+)$	0	$(4.97 \pm 0.03) \times 10^{2}$	$3.00^{+0.04}_{-0.04} \times 10^{1}$	0.060 ± 0.001

TABLE I. (*Continued.*)

Reaction	Q_α^{expt} (MeV)	J_i^π	J_f^π	ℓ_{min}	$T_{1/2}^{expt}$ (s)	$T_{1/2}^{calc}$ (s)	S_α
$^{203}At \to {}^{199}Bi + \alpha$	6.210 ± 0.001	$9/2^-$	$9/2^-$	0	$(1.43 \pm 0.04) \times 10^3$	$1.21^{+0.01}_{-0.01} \times 10^2$	0.084 ± 0.002
$^{204}At \to {}^{200}Bi + \alpha$	6.070 ± 0.001	7^+	7^+	0	$(1.40 \pm 0.02) \times 10^4$	$4.93^{-0.06}_{+0.06} \times 10^2$	0.035 ± 0.001
$^{205}At \to {}^{201}Bi + \alpha$	6.020 ± 0.002	$9/2^-$	$9/2^-$	0	$(1.61 \pm 0.05) \times 10^4$	$8.15^{+0.15}_{-0.15} \times 10^2$	0.051 ± 0.002
$^{206}At \to {}^{202}Bi + \alpha$	5.887 ± 0.005	$(5)^+[6^{+*},7^{+*}]$	5^+	0[2*]	$(2.04 \pm 0.05) \times 10^5$	$3.30^{+0.19}_{-0.18} \times 10^3$	0.016 ± 0.001
$^{207}At \to {}^{203}Bi + \alpha$	5.872 ± 0.003	$9/2^-$	$9/2^-$	0	$(7.58 \pm 0.13) \times 10^4$	$3.77^{+0.13}_{-0.12} \times 10^3$	0.050 ± 0.002
$^{208}At \to {}^{204}Bi + \alpha$	5.751 ± 0.002	6^+	6^+	0	$(1.07 \pm 0.02) \times 10^6$	$1.42^{+0.04}_{-0.04} \times 10^4$	0.013 ± 0.001
$^{209}At \to {}^{205}Bi + \alpha$	5.757 ± 0.002	$9/2^-$	$9/2^-$	0	$(4.75 \pm 0.04) \times 10^5$	$1.28^{+0.03}_{-0.03} \times 10^4$	0.027 ± 0.001
$^{210}At \to {}^{206}Bi + \alpha$	5.631 ± 0.001	$(5)^{+\dagger}$	6^+	2	$(1.67 \pm 0.08) \times 10^7$	$9.87^{+0.12}_{-0.12} \times 10^4$	0.006 ± 0.001
$^{211}At \to {}^{207}Bi + \alpha$	5.982 ± 0.001	$9/2^-$	$9/2^-$	0	$(6.21 \pm 0.01) \times 10^4$	$9.92^{+0.14}_{-0.14} \times 10^2$	0.016 ± 0.001
$^{212}At \to {}^{208}Bi + \alpha$	7.817 ± 0.001	$(1^-)^\dagger$	5^+	5	$(3.14 \pm 0.02) \times 10^{-1}$	$1.22^{+0.01}_{-0.01} \times 10^{-3}$	0.004 ± 0.001
$^{213}At \to {}^{209}Bi + \alpha$	9.254 ± 0.005	$9/2^-$	$9/2^-$	0	$(1.25 \pm 0.06) \times 10^{-7}$	$1.01^{+0.03}_{-0.03} \times 10^{-8}$	0.081 ± 0.004
$^{214}At \to {}^{210}Bi + \alpha$	8.987 ± 0.004	1^-	1^-	0	$(5.58 \pm 0.10) \times 10^{-7}$	$4.22^{+0.10}_{-0.09} \times 10^{-8}$	0.076 ± 0.002
$^{215}At \to {}^{211}Bi + \alpha$	8.178 ± 0.004	$9/2^-$	$9/2^-$	0	$(1.00 \pm 0.20) \times 10^{-4}$	$5.47^{+0.15}_{-0.14} \times 10^{-6}$	0.055 ± 0.011
$^{216}At \to {}^{212}Bi + \alpha$	7.950 ± 0.003	1^-	$1^{(-)}$	0	$(3.00 \pm 0.30) \times 10^{-4}$	$2.43^{+0.05}_{-0.05} \times 10^{-5}$	0.081 ± 0.008
$^{200}Fr \to {}^{196}At + \alpha$	7.620 ± 0.050	$(3^+)^\dagger$	(3^+)	0	$(4.90 \pm 0.40) \times 10^{-2}$	$4.9^{+2.2}_{-1.5} \times 10^{-3}$	0.107 ± 0.039
$^{201}Fr \to {}^{197}At + \alpha$	7.520 ± 0.050	$(9/2^-)$	$(9/2^-)$	0	$(6.20 \pm 0.50) \times 10^{-2}$	$1.01^{+0.48}_{-0.32} \times 10^{-2}$	0.175 ± 0.066
$^{202}Fr \to {}^{198}At + \alpha$	7.389 ± 0.004	$(3^+)^\dagger$	(3^+)	0	$(3.00 \pm 0.50) \times 10^{-1}$	$2.71^{+0.09}_{-0.08} \times 10^{-2}$	0.090 ± 0.015
$^{203}Fr \to {}^{199}At + \alpha$	7.275 ± 0.004	$(9/2^-)$	$(9/2^-)$	0	$(5.50 \pm 0.10) \times 10^{-1}$	$6.51^{+0.22}_{-0.21} \times 10^{-2}$	0.119 ± 0.004
$^{204}Fr \to {}^{200}At + \alpha$	7.170 ± 0.003	$(3^+)^\dagger$	(3^+)	0	$(1.96 \pm 0.33) \times 10^0$	$1.48^{+0.03}_{-0.03} \times 10^{-1}$	0.076 ± 0.013
$^{205}Fr \to {}^{201}At + \alpha$	7.055 ± 0.002	$(9/2^-)$	$(9/2^-)$	0	$(4.03 \pm 0.04) \times 10^0$	$3.79^{+0.08}_{-0.08} \times 10^{-1}$	0.094 ± 0.002
$^{206}Fr \to {}^{202}At + \alpha$	6.923 ± 0.004	$(2^+,3^+)[7^{+*}]$	$(2^+,3^+)$	0[4*]	$(1.60 \pm 0.01) \times 10^1$	$1.14^{+0.04}_{-0.04} \times 10^0$	0.088 ± 0.003
$^{207}Fr \to {}^{203}At + \alpha$	6.893 ± 0.002	$9/2^-$	$9/2^-$	0	$(1.56 \pm 0.01) \times 10^1$	$1.44^{+0.03}_{-0.03} \times 10^0$	0.092 ± 0.002
$^{208}Fr \to {}^{204}At + \alpha$	6.785 ± 0.024	7^+	7^+	0	$(6.64 \pm 0.03) \times 10^1$	$3.64^{+0.88}_{-0.71} \times 10^0$	0.056 ± 0.012
$^{209}Fr \to {}^{205}At + \alpha$	6.777 ± 0.004	$9/2^-$	$9/2^-$	0	$(5.67 \pm 0.08) \times 10^1$	$3.78^{+0.14}_{-0.13} \times 10^0$	0.067 ± 0.003
$^{210}Fr \to {}^{206}At + \alpha$	6.672 ± 0.005	6^+	$(5)^+$	2	$(2.69 \pm 0.05) \times 10^2$	$1.75^{+0.08}_{-0.08} \times 10^1$	0.065 ± 0.003
$^{211}Fr \to {}^{207}At + \alpha$	6.662 ± 0.003	$9/2^-$	$9/2^-$	0	$(2.14 \pm 0.01) \times 10^2$	$1.02^{+0.03}_{-0.03} \times 10^1$	0.048 ± 0.001
$^{212}Fr \to {}^{208}At + \alpha$	6.529 ± 0.002	5^+	6^+	2	$(2.79 \pm 0.08) \times 10^3$	$6.31^{+0.10}_{-0.10} \times 10^1$	0.023 ± 0.001
$^{213}Fr \to {}^{209}At + \alpha$	6.905 ± 0.001	$9/2^-$	$9/2^-$	0	$(3.50 \pm 0.01) \times 10^1$	$1.06^{+0.01}_{-0.01} \times 10^0$	0.030 ± 0.001
$^{214}Fr \to {}^{210}At + \alpha$	8.589 ± 0.004	$(1^-)^\dagger$	$(5)^+$	5	$(5.00 \pm 0.20) \times 10^{-3}$	$3.95^{+0.10}_{-0.10} \times 10^{-5}$	0.008 ± 0.001
$^{215}Fr \to {}^{211}At + \alpha$	9.540 ± 0.007	$9/2^-$	$9/2^-$	0	$(8.60 \pm 0.50) \times 10^{-8}$	$1.04^{+0.04}_{-0.04} \times 10^{-8}$	0.122 ± 0.008
$^{216}Fr \to {}^{212}At + \alpha$	9.174 ± 0.003	$(1^-)^\dagger$	(1^-)	0	$(7.00 \pm 0.20) \times 10^{-7}$	$7.29^{+0.12}_{-0.12} \times 10^{-8}$	0.104 ± 0.003
$^{217}Fr \to {}^{213}At + \alpha$	8.469 ± 0.004	$9/2^-$	$9/2^-$	0	$(1.90 \pm 0.30) \times 10^{-5}$	$4.66^{+0.12}_{-0.12} \times 10^{-6}$	0.245 ± 0.039
$^{218}Fr \to {}^{214}At + \alpha$	8.014 ± 0.002	1^-	1^-	0	$(1.00 \pm 0.60) \times 10^{-3}$	$9.21^{+0.13}_{-0.13} \times 10^{-5}$	0.092 ± 0.055
$^{219}Fr \to {}^{215}At + \alpha$	7.449 ± 0.002	$9/2^-$	$9/2^-$	0	$(2.00 \pm 0.20) \times 10^{-2}$	$5.67^{+0.08}_{-0.08} \times 10^{-3}$	0.266 ± 0.034
$^{220}Fr \to {}^{216}At + \alpha$	6.801 ± 0.002	1^+	1^-	1	$(2.75 \pm 0.03) \times 10^1$	$1.51^{+0.03}_{-0.03} \times 10^0$	0.055 ± 0.001
$^{221}Fr \to {}^{217}At + \alpha$	6.458 ± 0.001	$5/2^-$	$9/2^-$	2	$(2.86 \pm 0.01) \times 10^2$	$5.35^{+0.07}_{-0.07} \times 10^1$	0.187 ± 0.003
$^{206}Ac \to {}^{202}Fr + \alpha$	7.940 ± 0.050	$(3^+)^\dagger$	(3^+)	0	$(2.20 \pm 0.90) \times 10^{-2}$	$2.5^{+1.1}_{-0.8} \times 10^{-3}$	0.122 ± 0.065
$^{207}Ac \to {}^{203}Fr + \alpha$	7.840 ± 0.050	$(9/2^-)^\dagger$	$(9/2^-)$	0	$(2.7 \pm 1.1) \times 10^{-2}$	$5.0^{+2.3}_{-1.6} \times 10^{-3}$	0.20 ± 0.11
$^{208}Ac \to {}^{204}Fr + \alpha$	7.730 ± 0.050	$(3^+)[7^{+*}]$	(3^+)	0[4*]	$(9.6 \pm 2.4) \times 10^{-2}$	$1.11^{+0.51}_{-0.35} \times 10^{-2}$	0.124 ± 0.055
$^{209}Ac \to {}^{205}Fr + \alpha$	7.730 ± 0.050	$(9/2^-)^\dagger$	$(9/2^-)$	0	$(1.01 \pm 0.51) \times 10^{-1}$	$1.07^{+0.49}_{-0.34} \times 10^{-2}$	0.114 ± 0.070
$^{210}Ac \to {}^{206}Fr + \alpha$	7.610 ± 0.050	$(7^+)^\dagger$	(7^+)	0	$(3.85 \pm 0.55) \times 10^{-1}$	$2.6^{+1.2}_{-0.8} \times 10^{-2}$	0.073 ± 0.029
$^{211}Ac \to {}^{207}Fr + \alpha$	7.620 ± 0.050	$(9/2^-)^\dagger$	$9/2^-$	0	$(2.10 \pm 0.30) \times 10^{-1}$	$2.3^{+1.1}_{-0.7} \times 10^{-2}$	0.119 ± 0.047
$^{212}Ac \to {}^{208}Fr + \alpha$	7.520 ± 0.050	$(6^+)^\dagger$	7^+	2	$(1.63 \pm 0.09) \times 10^0$	$8.8^{+4.3}_{-2.9} \times 10^{-2}$	0.058 ± 0.022
$^{213}Ac \to {}^{209}Fr + \alpha$	7.500 ± 0.050	$(9/2^-)^\dagger$	$9/2^-$	0	$(7.38 \pm 0.16) \times 10^{-1}$	$5.5^{+2.7}_{-1.8} \times 10^{-2}$	0.081 ± 0.031
$^{214}Ac \to {}^{210}Fr + \alpha$	7.352 ± 0.003	$(5^+)^\dagger$	6^+	2	$(9.21 \pm 0.23) \times 10^0$	$3.17^{+0.08}_{-0.08} \times 10^{-1}$	0.034 ± 0.001
$^{215}Ac \to {}^{211}Fr + \alpha$	7.746 ± 0.003	$9/2^-$	$9/2^-$	0	$(1.70 \pm 0.10) \times 10^{-1}$	$7.77^{+0.18}_{-0.17} \times 10^{-3}$	0.046 ± 0.003

Here $k(R)$ is the relative-motion momentum given by

$$k^2(R) = \frac{2\mu}{\hbar^2}[E_{\rm c.m.} - V_N(E,R) - V_C(R)], \quad (9)$$

where $E_{\rm c.m.}$ is the center-of-mass (c.m.) energy. $V_N(E,R) = V_D(E,R) + V_{Ex}(E,R)$ and $V_C(R)$ are the total nuclear and Coulomb potentials, respectively. The folded potential is energy dependent and nonlocal through its exchange term and contains a self-consistency problem because the relative-motion momentum, $k(R)$, depends upon the total nuclear potential, $V_N(E,R) = V_D(E,R) + V_{Ex}(E,R)$, itself. This problem is solved by the iteration method. The exact treatment of the nonlocal exchange term is complicated numerically, but one may obtain an equivalent *local* potential by using a realistic localized expression for the nonlocal density matrix (DM) [40].

Following the work of Refs. [41–43], one easily obtains the self-consistent and local exchange potential V_{Ex} as

$$V_{\rm Ex}(E,R) = 4\pi \int_0^\infty ds\, s^2\, \upsilon_{Ex}(\rho,E,s)\, j_0(k(R)s/M) \times \int d\vec{y}\rho_d(|\vec{y}-\vec{R}|)\, \hat{j}_1(k_{\rm eff}(|\vec{y}-\vec{R}|)s) \times \rho_\alpha(y)\exp\left(-\frac{s^2}{4b_\alpha^2}\right). \quad (10)$$

The local Fermi momentum $k_{\rm eff}(r)$ is given by [40,41]

$$k_{\rm eff}(r) = \left\{\frac{5}{3\rho(r)}\left[\tau(r) - \frac{1}{4}\nabla^2\rho(r)\right]\right\}^{1/2}. \quad (11)$$

The kinetic energy density is then given by

$$\tau(r) = \frac{3}{5}\left(\frac{3\pi^2}{2}\right)^{2/3}\rho(r)^{5/3} + \frac{1}{3}\nabla^2\rho(r) + \frac{1}{36}\frac{|\vec{\nabla}\rho(r)|^2}{\rho(r)}. \quad (12)$$

A realistic NN interaction is used in our calculations whose parameters reproduce consistently the equilibrium density and the binding energy of normal nuclear matter as well as the density and energy dependence of the nucleon-nucleus optical potential. The density dependent M3Y-Paris effective NN interaction, CDM3Y1, has been adopted in the present work as described in Ref. [41].

Finally, the obtained α-daughter interaction potential is employed to compute the barrier penetrability, Eq. (2), and the assault frequency, Eq. (3), which are used in turn to obtain the decay half-life time. Now, the calculated half-lives, without S_α, and the experimental ones allow for deducing the spectroscopic factor of the α cluster inside the parent nucleus as [27,33]

$$S_\alpha = T_{1/2}^{\rm calc}/T_{1/2}^{\rm expt}. \quad (13)$$

III. RESULTS AND DISCUSSION

The interaction potential between the α particle and daughter nucleus plays an important role in the theoretical calculation of the penetration probability and half-life of α decay; the calculation of this potential becomes important in describing the decay process. In the present study, we have constructed the microscopic α-nucleus potential numerically in the well-established double-folding model for both Coulomb and nuclear potentials. A realistic density-dependent CDM3Y1 interaction, based on the G-matrix elements of the Paris NN potential, has been used in the folding calculation. In contrast to the other traditional semiclassical approximations which ignore the main effect of antisymmetrization under exchange of nucleons between the α and the daughter nuclei, the present calculations took into account such an effect in the folding model through the finite-range exchange part of the NN interaction. The local approximation for the nondiagonal one-body density matrix in the calculation of the exchange potential was included by using the harmonic oscillator representation of the nondiagonal density matrix of the α particle.

In a series of articles [9,24–26], we investigated the correlation between the variation of α-particle preformation probability, S_α, with the neutron number for isotopes of an element and the neutrons and protons energy levels of the parent nucleus occupied by the emitted α particle. This correlation was done for even-even and even-odd nuclei in the range $74 \leqslant Z \leqslant 102$. We found that S_α has a regular behavior with the N variation if the neuron pair in the α particle, emitted from adjacent isotopes, comes from the same energy level or from a group of levels assuming that the order of levels in this group is not changed. Irregular behavior of S_α with N occurs if the levels of the adjacent isotopes change or holes are created in lower levels. Based on the similarity in the behavior of S_α with N for two adjacent nuclei, we predicted and confirmed the unknown or doubted spin and parity for the considered nuclei.

In the present analysis, we assume that the states of the parent nucleus consist of a few valence configurations which determine its spin and parity in the framework of the shell model. The level sequences and occupation number of levels are deduced from the spin and parity assignments of the parent and daughter nuclei and, in some cases, they are confirmed by the tabulated values of J^π of the neighboring isotopes and/or isotones of the parent nucleus. We consider, in the present study, the odd-even and odd-odd nuclei with $77 \leqslant Z \leqslant 89$. Two rules [44] are used to determine the total spin of odd-odd isotopes. The first is the strong rule given by $J = |j_p - j_n|$ if $j_p = \ell_p \pm \frac{1}{2}$ and $j_n = \ell_n \mp \frac{1}{2}$. The other rule is the weak rule given by $J = j_p + j_n$ if $j_p = \ell_p \pm \frac{1}{2}$ and $j_n = \ell_n \pm \frac{1}{2}$. The weak rule is frequently given in the less specific form $|j_p - j_n| < J \leqslant j_p + j_n$. j_p and ℓ_p (or j_n and ℓ_n) represent the total and orbital angular momenta of the odd proton (or neutron). In the present work, a useful measure for the average strength of the proton-neutron interaction is used which plays an important role in the behavior of S_α. It is given by the average value [45–47] $f_{np} = (\frac{1}{1+\triangle n+\triangle\ell+\triangle j})_{\rm avg}$, where $\triangle n$, $\triangle\ell$, and $\triangle j$ are the differences in quantum numbers n, ℓ, and j, respectively, of the levels occupied by protons and neutrons. The average is taken over the two protons' and two neutrons' energy levels.

Figure 1 shows the neutron number variation of S_α for both even and odd neutron number isotopes of Ir ($Z = 77$). The value of the α-emission preformation probability, S_α, varies strongly with the neutron number, which indicates that the neutron levels, proton levels, or both change rapidly as N increases. For $N = 100$, the spin of the isotope ^{177}Ir is

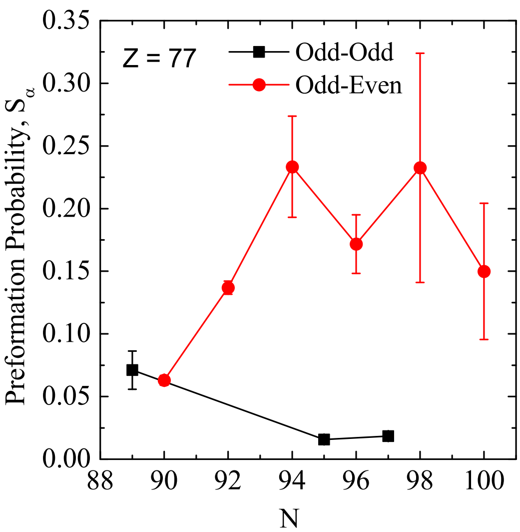

FIG. 1. Extracted α-preformation probability, S_α, for different Ir isotopes ($Z = 77$) with the parent neutron number N.

confirmed and it has a value $J^\pi = 5/2^-$, indicating that the unpaired proton exists in the $2f_{5/2}$ level. Another confirmed spin is for the ^{167}Ir isotope with $N = 90$: it has $J^\pi = 1/2^+$ (proton occupies the $3s_{1/2}$ level). The proton levels $2d_{5/2}$, $2d_{3/2}$, and $1h_{11/2}$ also appear in the tabulated spins of the odd-even Ir isotopes. For neutron levels, the $2f_{7/2}$ level is filled by neutrons at $N = 100$ and we found that the levels $3p_{3/2}$, $2f_{5/2}$, and $3p_{1/2}$ contribute to α emission for the odd neutron number isotopes of the elements Pt ($Z = 78$) and Os ($Z = 76$) [26]. We also found that the level $1i_{13/2}$ can contribute to the emission process, leaving holes in the lower neutron levels. For $N = 100$, the value of S_α is about 0.150 ± 0.054, and J^π for the ^{177}Ir isotope is $5/2^-$. Thus the unpaired proton exists in the $2f_{5/2}$ level and the neutron pair in the α-particle comes from $2f_{7/2}$ level. The measure of n-p interaction in this case is $f_{np} = 1/2$ which is too large, which explains the small value of S_α. For $N = 98$, the value of S_α is about 0.233 ± 0.091, indicating that the value of f_{np} is reduced. This can be satisfied by assuming that the neutron pair comes from $1i_{13/2}$ level. In this case, $f_{np} = 0.11$. For $N = 96$, the tabulated spin value is $3/2^+$ or $5/2^+$ and $S_\alpha \simeq 0.172 \pm 0.023$, the odd proton is in the $2d_{3/2}$ or $2d_{5/2}$ levels, and the neutron pair in the α particle occupies the $2f_{7/2}$ level ($f_{np} = 0.33$ if the proton level is $2d_{5/2}$ and $f_{np} = 0.25$ for the $2d_{3/2}$ level). Since the value of S_α is small, we choose the proton level $2d_{5/2}$. At $N = 94$, S_α increases to 0.233 ± 0.040 and $J^\pi = 11/2^-$, indicating that the level $1h_{11/2}$ contributes to the emission. The value of f_{np} is too small, thus the proton pair occupies the $1h_{11/2}$ level and the neutron pair exists in the $2f_{5/2}$ level (the J^π value of ^{171}Os is $5/2^-$). This reduces the value of f_{np} to 1/7, producing a large value of S_α. For $N = 97$, the tabulated spin is $J^\pi = 3^+$, the odd proton may exist in the $1h_{11/2}$ level, and the unpaired neutron occupies the $2f_{5/2}$ level; the coupled spin according to the strong coupling rule is $J = 11/2 - 5/2 = 3^+$ which agrees with the tabulated spin value and the value of f_{np}, in this case, is 1/7. Since the value of S_α is too small, the emission levels of proton and neutron pairs are probably $1h_{11/2}$ and $1i_{13/2}$, respectively. In this case, f_{np} is equal to 1/3. The point $N = 95$ is the same as $N = 97$, indicating that the levels for these two neutron values are the same. For $N = 92$, $J^\pi = 1/2^+$ and the unpaired proton exists in the $3s_{1/2}$ level while the neutron may be in the level $2f_{5/2}$ (J^π of ^{169}Os is $5/2^-$). The proton pair is emitted from two different levels. The same level sequences exist at $N = 90$ since the difference in the values of S_α at $N = 90$ and $N = 92$ is small. For $N = 89$, S_α is almost the same as $N = 90$, thus the odd proton and the odd neutron exist in the levels $3s_{1/2}$ and $2f_{5/2}$, respectively, and couple to $J^\pi = 2^-$.

Figure 2(a) is the same as Fig. 1 except it is for the Au ($Z = 79$) isotopes. For the odd-even Au isotopes, the following tabulated spins appear: $J^\pi = 5/2^-$, $3/2^-$, $3/2^+$, and $1/2^+$ indicating that the unpaired proton has the levels $2f_{5/2}$, $3p_{3/2}$, $2d_{3/2}$, and $3s_{1/2}$, respectively. The level $3p_{3/2}$ is excluded since it appears at $Z = 99$ [48]. For $N = 106$, the proton pair occupies the $2f_{5/2}$ level and the neutron pair occupies the $1i_{13/2}$ level (J^π for ^{187}Pb with $N = 105$ is $13/2^+$). If proton pair and neutron pair in α particle come from the above mentioned levels, the neutron-proton interaction will be small due to the large differences in quantum numbers between the two levels and S_α will be large. For $N = 107$, the confirmed spin of the odd-odd ^{186}Au isotope is 3^-, and S_α for this point is reduced strongly due to the change in the proton and neutron level sequences. The value $J^\pi = 3^-$ can be obtained from the weak rule of coupling spins if the unpaired proton is in the $3s_{1/2}$ level and the unpaired neutron is in the $2f_{5/2}$ level. Since one proton occupies the $3s_{1/2}$ level then the proton pair comes from two different levels. For $N = 105$, the confirmed spin of ^{184}Au isotope is 5^+ coming from coupling of spins of the proton in the $2d_{3/2}$ level and the neutron in the $1i_{13/2}$ level. f_{np}, in this case, has the value of 1/12. For $N = 104$, the proton is in the $2f_{5/2}$ level and the neutron is in the $3p_{3/2}$ level (J^π for ^{185}Pb is $3/2^-$ [48]). For $N = 102$, the proton exists in the $2f_{5/2}$ level and the neutron exists in the $3p_{1/2}$ level (J^π for Hg with $A = 181$, 183, and 185 is $1/2^-$ [48]). It should be noted that the value of f_{np} for the two levels $2f_{5/2}$ and $3p_{3/2}$ is 0.2, while its value is 0.167 for the $2f_{5/2}$ and $3p_{1/2}$ levels. For $N = 100$, the odd proton occupies the $3s_{1/2}$ level while the neutron exists in the $1i_{13/2}$. The large reduction in the neutron-proton interaction causes a jump in the value of S_α. For $N = 98$, 94, and 91, the values of S_α are almost the same ($S_\alpha \simeq 0.07$), indicating that α decay happens from the same levels. The neutron-proton interaction is large for the above mentioned neutron values while S_α has a small value. The proton for the three points exists in the $3s_{1/2}$ level while the neutron exists in the $3p_{3/2}$.

Table II lists the experimental Q values with their uncertainties, as obtained in Ref. [49]. The experimental half-lives with their asymmetric uncertainties and the values of spin and parities of the ground states of parent nuclei are obtained from Ref. [50] for Au isotopes. The calculated α decay-half lives with their asymmetric uncertainties and the extracted preformation factors with their uncertainties are also presented. We also displayed in Fig. 2(b) the extracted α preformation factors with their uncertainties for different Au isotopes using the experimental data of Refs. [49,50] for comparison with our calculations using the updated experimental data of NNDC of Ref. [48]. The general trend of variation of preformation factor

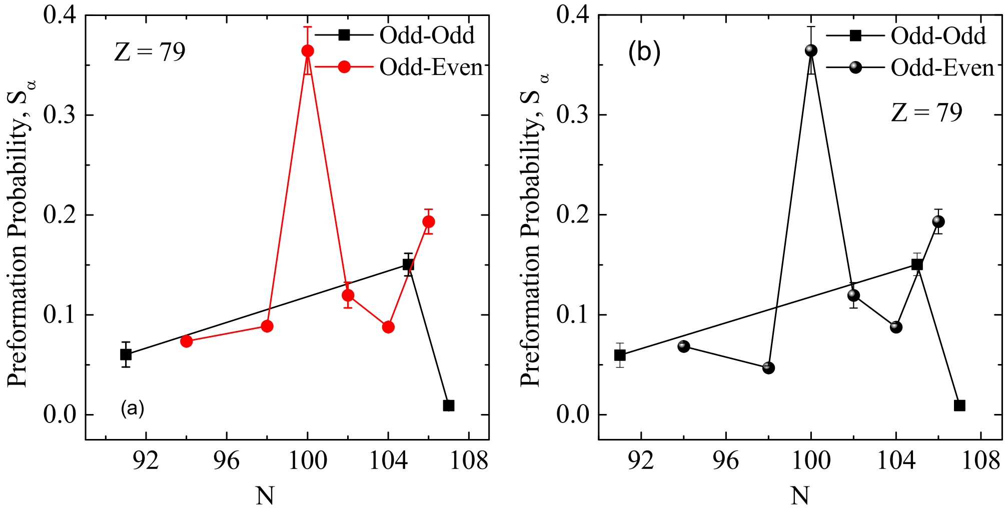

FIG. 2. The same as Fig. 1 but for Au isotopes. Panel (b) presents the extracted alpha preformation factors with their uncertainties for different Au isotopes using the experimental data of Refs. [49,50]

is almost the same in the two figures, which does not affect our conclusion on the nuclear spin and parities.

The α emitters of the Tl ($Z = 81$) isotopes are only four isotopes with $N = 96$, 98, 100, and 99. S_α values are, respectively, 0.084 ± 0.024, 0.154 ± 0.028, 0.033 ± 0.004, and 0.002 ± 0.001. The tabulated spin for the even neutron number isotopes is $1/2^+$; this value does not change by emission. Thus, the proton pair in the α decay comes from other occupied levels below the level $3s_{1/2}$. The change in S_α is due to change in the neutron levels. The neutron pair may come from the $2f_{7/2}$ level at $N = 96$ and 100. At $N = 98$, the neutron pair comes from the $1i_{13/2}$ level; this is why the value of S_α is large at $N = 98$. For the odd-odd ^{180}Tl isotope, the tabulated spin is 4^- or 5^-. The value of $J^\pi = 4^-$ can be obtained by strong coupling rule of the proton in the $3s_{1/2}$ level and the neutron in the $2f_{7/2}$ level; the other spin value, $J^\pi = 5^-$, cannot be obtained from the proton and neutron levels considered in the neighboring elements $Z = 77$ and 79. Thus, we confirm $J^\pi = 4^-$ for ^{180}Tl.

Figure 3 shows our results of α-preformation probability for the Bi ($Z = 83$) isotopes. For even neutron number Bi isotopes, the odd proton occupies the proton level $1h_{9/2}$, which exists above the closed shell $Z = 82$. The upper level in this closed shell is $3s_{1/2}$. The proton pair in the α particle for the odd mass number Bi isotopes with neutron numbers $N = 104$–112 comes from the two levels $1h_{9/2}$ and $3s_{1/2}$, as discussed in Ref. [26]. When the proton pair is emitted from the parent nucleus, it leaves the daughter nucleus with spin $J^\pi = 1/2^+$. When the neutron number is decreased to $N = 102$, the confirmed spin of the parent nucleus becomes $1/2^+$ and the proton pair comes from the level $1h_{9/2}$. As discussed in Ref. [26], the neutron pair in the emitted α particle for Bi isotopes with $N = 112$, 110, and 106 comes from the level $3p_{3/2}$. For $N = 108$, the increase in S_α is due to the

TABLE II. The preformation probability, S_α, and the α-decay half-lives, $T_{1/2}^{\rm calc}$, calculated without S_α Au isotopes using the CDM3Y1-Paris NN interaction. Experimental Q values with their uncertainties are taken from Ref. [49]. The experimental partial half-life is extracted by using the experimental half-life and the intensity given in Ref. [50]. Presented in the third and fourth columns are the spin and parity of the ground states of parent (column 3) and daughter (column 4) nuclei, respectively obtained from Ref. [50]. Uncertain spin and/or parity assignments are in parentheses. The sign * means the spin and/or parity assignments as well as the angular momentum of transition are modified according to the behavior of S_α and their modified values are in brackets beside the values used in our calculations. The sign † means the tabulated spin is confirmed by the behavior of S_α.

Reaction	$Q_\alpha^{\rm expt}$ (MeV)	J_i^π	J_f^π	$\ell_{\rm min}$	$T_{1/2}^{\rm expt}$ (s)	$T_{1/2}^{\rm calc}$ (s)	S_α
^{170}Au $\rightarrow$ ^{166}Ir $+ \alpha$	7.177 ± 0.015	$(2^-)^\dagger$	(2^-)	0	$(2.64 \pm 0.46) \times 10^{-3}$	$1.56^{+0.18}_{-0.16} \times 10^{-4}$	0.060 ± 0.012
^{173}Au $\rightarrow$ ^{169}Ir $+ \alpha$	6.836 ± 0.005	$(1/2^+)^\dagger$	$(1/2^+)$	0	$(2.91 \pm 0.12) \times 10^{-2}$	$1.96^{+0.08}_{-0.03} \times 10^{-3}$	0.068 ± 0.003
^{177}Au $\rightarrow$ ^{173}Ir $+ \alpha$	6.298 ± 0.004	$(1/2^+)^\dagger$,$(3/2^+)$	$(1/2^+,3/2^+)$	0	$(3.65 \pm 0.08) \times 10^{0}$	$1.71^{+0.06}_{-0.06} \times 10^{-1}$	0.047 ± 0.002
^{179}Au $\rightarrow$ ^{175}Ir $+ \alpha$	5.981 ± 0.005	$(1/2^+)^\dagger$,$(3/2^+)$	$(5/2^-)$	3	$(3.23 \pm 0.14) \times 10^{1}$	$1.18^{+0.06}_{-0.06} \times 10^{1}$	0.365 ± 0.024
^{181}Au $\rightarrow$ ^{177}Ir $+ \alpha$	5.751 ± 0.003	$(3/2^-)[5/2^{-*}]$	$5/2^-$	2[0*]	$(5.07 \pm 0.52) \times 10^{2}$	$6.05^{+0.19}_{-0.18} \times 10^{1}$	0.119 ± 0.013
^{183}Au $\rightarrow$ ^{179}Ir $+ \alpha$	5.465 ± 0.003	$5/2^-$	$(5/2)^-$	0	$(7.78 \pm 0.18) \times 10^{3}$	$6.82^{+0.23}_{-0.22} \times 10^{2}$	0.088 ± 0.004
^{184}Au $\rightarrow$ ^{180}Ir $+ \alpha$	5.234 ± 0.005	5^+	$(4,5)^{(+)}$	2	$(1.29 \pm 0.06) \times 10^{5}$	$1.93^{+0.12}_{-0.11} \times 10^{4}$	0.150 ± 0.011
^{185}Au $\rightarrow$ ^{181}Ir $+ \alpha$	5.180 ± 0.005	$5/2^-$	$5/2^-$	0	$(9.81 \pm 0.14) \times 10^{4}$	$1.89^{+0.12}_{-0.11} \times 10^{4}$	0.193 ± 0.012
^{186}Au $\rightarrow$ ^{182}Ir $+ \alpha$	4.912 ± 0.014	3^-	3^+	1	$(8.03 \pm 0.38) \times 10^{7}$	$7.25^{+1.51}_{-1.24} \times 10^{5}$	0.009 ± 0.002

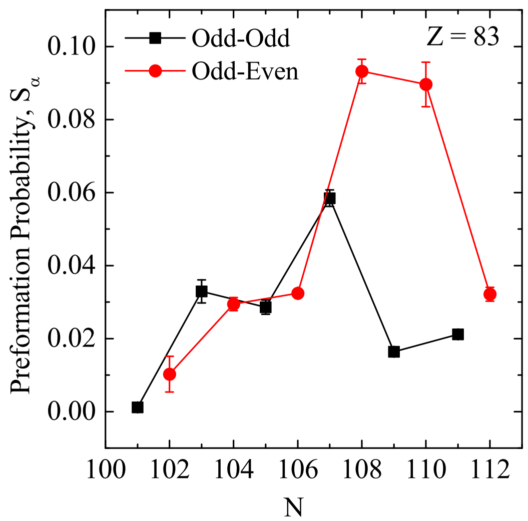

FIG. 3. The same as Fig. 1 but for Bi isotopes.

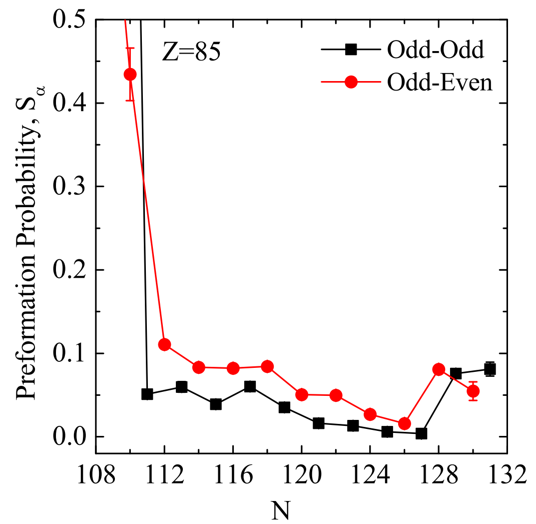

FIG. 4. The same as Fig. 1 but for At isotopes.

contribution of the neutron level $1i_{13/2}$ to the emission process (the neutron levels in this neutron range are similar to Po levels in the same neutron number range [9,24]). The $3p_{3/2}$ level is filled by neutrons several times to contribute again at $N = 102$ to the α emission. It should be noted that the measure of f_{np} for $N = 102$, 106, 110, and 112 is 0.217 and is reduced to 0.158 at $N = 104$ and 108.

For odd neutron number isotopes of Bi, Fig. 3 shows that the behavior of S_α is quite similar to that for even neutron number isotopes. This means that the levels of Bi isotopes do not change when a neutron is added in the neutron range $N = 101$–111. For the neutron values 111, 109, 105, and 101, the unpaired proton exists in the level $1h_{9/2}$ and the unpaired neutron occupies the level $3p_{3/2}$; the two nucleons couple to spin 3^+ using the strong rule. After the emission, the unpaired neutron (proton) exists in the level $3p_{3/2}$ ($3s_{1/2}$); they couple their spins to 2^-. For $N = 103$ and 107, the unpaired neutron (proton) exists in the level $1i_{13/2}$ ($1h_{9/2}$); they couple their spins to 2^-. After the emission, the unpaired neutron (proton) occupies the level $1i_{13/2}$ ($3s_{1/2}$); they couple their spins to 7^+. Thus, the variation of S_α predicts the spin value 3^+ for Bi isotopes with neutron numbers $N = 101$, 105, 109, and 111 while $J^\pi = 2^-$ for $N = 103$ and 107.

Figure 4 shows the neutron variation of S_α for At isotopes with odd and even neutron numbers. The figure shows almost similarity of S_α for even-odd and odd-odd isotopes. This means that the addition of a neutron to odd-even isotopes does not affect their level sequences. For At with even neutron numbers in the range $112 \leqslant N \leqslant 130$, the unpaired proton occupies the $1h_{9/2}$ level; this is clear since J^π values in this neutron variation range for the parent and daughter nuclei are $9/2^-$. Thus we confirm the value $J^\pi = 9/2^-$ for parent and daughter nuclei with neutron numbers in the range $112 \leqslant N \leqslant 130$. For $N = 126$, 128, and 130, the upper occupied neutron levels are $3p_{1/2}$, $2g_{9/2}$, and $2g_{9/2}$, respectively. This is reasonable since the spin of odd neutron number isotopes of Po ($Z = 84$) is $9/2^+$ for the N values 127, 129, and 131. Thus, for $N = 126$, 128, and 130 isotopes of At, the two protons of the emitted α particle come from the $1h_{9/2}$ level and the two neutrons come from the $2g_{9/2}$ level (for $N = 130$ and 128) and from the $3p_{1/2}$ level for $N = 126$. This change in the neutron levels causes a decrease in S_α at $N = 126$. For the odd neutron number isotopes with $N = 127$, 129, and 131, the odd proton exists in $1h_{9/2}$ level and the odd neutron occupies $2g_{9/2}$; they couple their spins to 1^- (weak rule). For $N = 127$, emission occurs from the levels $1h_{9/2}$ (for protons) and $2g_{9/2}$ and $3p_{1/2}$ (for neutrons), thus the daughter nucleus has the resulting spin of coupling $1/2^-$ and $9/2^-$ which is 5^+, in agreement with the confirmed tabulated value. For $N = 129$ and 131, the unpaired nucleon does not change its level after emission, so the spin of daughter nucleus is 1^-. For $N = 125$, remembering that the unpaired proton is in the $1h_{9/2}$ level, the unpaired neutron exists in the $3p_{1/2}$ level and as in Po [9] the emitted neutrons come from $3p_{1/2}$ and $2f_{5/2}$ levels. Thus J^π for the parent nucleus is 5^+ (strong rule) and for the daughter the confirmed value is 6^+ (rule $j_1 + j_2 - 1$).

Following the neutron level sequence of Po [9], for $N = 123$ the odd neutron is in the $2f_{5/2}$ level and $J_p^\pi = J_d^\pi = 6^+$ by the weak rule of coupling. For $N = 121$, the unpaired neutron exists in the level $2f_{5/2}$ (occupied by three neutrons) and the pair comes from the same level as $N = 123$ (S_α has almost the same value for $N = 121$ and 123) thus $J^\pi = 6^+$ or 7^+ as required by the Fr isotope with the same value of N (the confirmed spin value of ^{208}Fr is $J^\pi = 7^+$ as seen from Table I). For $N = 119$, the single neutron occupies the level $2f_{5/2}$ and the unpaired proton in the level $1h_{9/2}$ couples with the neutron to $J^\pi = 7^+$, which is confirmed. Emission of two neutrons does not change the level of the unpaired neutron, perhaps because the neutron pair comes from a lower level. For $N = 117$, the neutron pair comes from $3p_{3/2}$ and the proton in $1h_{9/2}$ couples to $3/2^-$ to give 3^+. For $N = 115$, 113, and 111, the emission of the neutron pair is from $3p_{3/2}$ level which is filled two times; the value of S_α is almost constant and its possible value of spin is 3^+. For $N < 111$, the spins of the odd-even isotopes change from $9/2^-$ to $1/2^+$, which means creation of a proton hole in $3s_{1/2}$ level. The neutron level $1i_{13/2}$ contributes

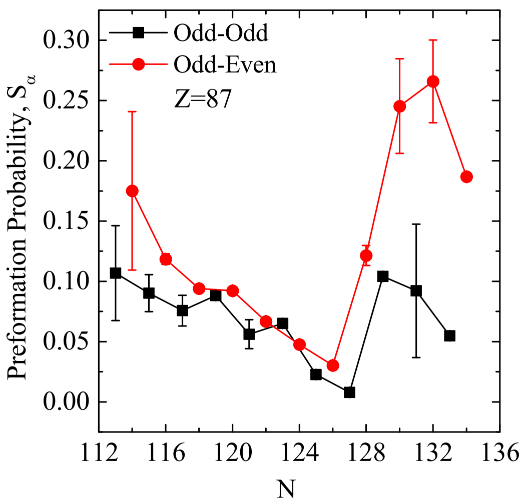

FIG. 5. The same as Fig. 1 but for Fr isotopes.

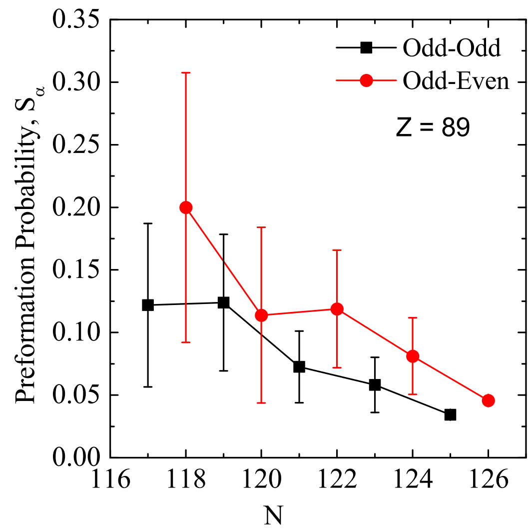

FIG. 6. The same as Fig. 1 but for Ac isotopes.

to emission, producing a jump in the value of S_α at $N = 106$, 108, 110, and 109. At $N = 109$, the odd proton in $3s_{1/2}$ couples with the odd neutron in $1i_{13/2}$ to produce 7^+.

Figure 5 shows the results for Fr ($Z = 87$) even and odd neutron number isotopes. At $N = 134$, $J^\pi = 5/2^-$, which means that the unpaired proton is in the level $2f_{5/2}$ while the level $1h_{9/2}$ has four protons. After decay, the level $1h_{9/2}$ has three protons and the spin of the daughter is $9/2^-$. For even neutron isotopes in the range $114 \leqslant N \leqslant 132$, the spins of the parent and daughter nuclei indicate that the odd proton exists in the $1h_{9/2}$ level. For Fr isotope with $N = 133$, the unpaired neutron and unpaired proton couple their spins to $J^\pi = 1^+$. This confirmed spin value can be obtained by assuming that the odd proton exists in the $2f_{5/2}$ level (the spin of ^{221}Fr isotope has the confirmed value $J^\pi = 5/2^-$) and the unpaired neutron occupies the $3p_{3/2}$ level. After decay, the daughter nucleus will be an At isotope with $N = 131$ (proton in $9/2^-$ level and neutron in $9/2^+$ level). The appearance of the $3p_{3/2}$ level at this large value of N causes a sudden increase in S_α at $N = 133$ and 134. The behavior of S_α for Fr isotopes at $N = 131$, 129, 127, and 125 is exactly the same as for At isotopes (Fig. 4) at the corresponding N values. Moreover, the corresponding values of S_α for the two elements are almost the same. Thus, the neutron and proton level sequences of Ac and Fr at $N = 131$, 129, 127, and 125 are the same. So we confirm the following spin values for Fr isotopes: ^{218}–214Fr have $J^\pi = 1^-$ and ^{212}Fr has $J^\pi = 5^+$. Comparing Fig. 5 for Fr and Fig. 4 for At isotopes, one can see almost similar behavior of S_α, in the two figures, at neutron numbers $113 \leqslant N \leqslant 125$, indicating that the level sequences of proton and neutron for the two elements At and Fr are the same in this neutron variation range. Thus, we confirm the spins of ^{206}Fr and $^{200-204}$Fr are, respectively, 7^+ and 3^+.

Figure 6 shows the neutron number variation of the α-particle preformation probability for the isotopes of the element Ac ($Z = 89$). For even neutron number isotopes, the values of S_α are in the range 0.046–0.200 with the smallest value of S_α at $N = 126$ and largest value at $N = 118$. Comparison of the behavior of S_α in the neutron variation range $N = 118$–126 for Ac with the corresponding quantities for Ra (Fig. 3 and Table I of Ref. [9]) shows that the behavior of S_α with neutron variation for Ac is almost the same as for Ra. Moreover, the values of S_α for Ra in this neutron variation range are almost equal to the corresponding values for Ac. This shows that for the isotopes with N values in the range $118 \leqslant N \leqslant 126$ the addition of one proton to Ra does not affect the level sequence, and the neutron and proton pairs in the α particle come from the same proton and neutron levels in the two adjacent elements. Since the unpaired proton exists in the $1h_{9/2}$ level, we can confirm the spin value $J^\pi = 9/2^-$ for odd-even Ac isotopes in the neutron variation range $118 \leqslant N \leqslant 126$.

For odd neutron number isotopes of Ac, S_α varies slowly with neutron number variation (from about 0.034 to 0.124). Its variation is almost similar to that of Fr shown on Fig. 5. Thus the spins of odd-odd Ac isotopes in the N-variation range $117 \leqslant N \leqslant 125$ are the same as the corresponding spins of Fr in the same neutron variation range. As in the case of Fr, the J^π values for odd-odd isotopes with $N = 117$, 119, 121, 123, and 125 are 3^+, 7^+, 7^+, 6^+, and 5^+, respectively.

Figure 7 displays the deviations of calculated α-decay half-lives from the experimental data as a function of the neutron number N of the parent nucleus for both odd-even and odd-odd nuclei. It is essential to evaluate the absolute α-decay half-lives with the inclusion of the α-preformation factor, S_α, which gives the probability that the α particle exists as a recognizable entity inside the nucleus before its emission. It is convenient and applicable to take a constant preformation factor for certain types of nuclei. The motivation for this is clearly shown in Refs. [51–53]. In the present study, we use the preformation probability $S_\alpha = 0.25$ for odd-A nuclei and $S_\alpha = 0.15$ for odd-odd nuclei, as indicated in Ref. [53].

It is clear that, for most of the decays, the deviation of calculated α decay half-lives with the corresponding experimental data lie within the order 2. This means that most of the calculated α decay half-lives are in good agreement with the experimental data for the studied nuclei. Because the

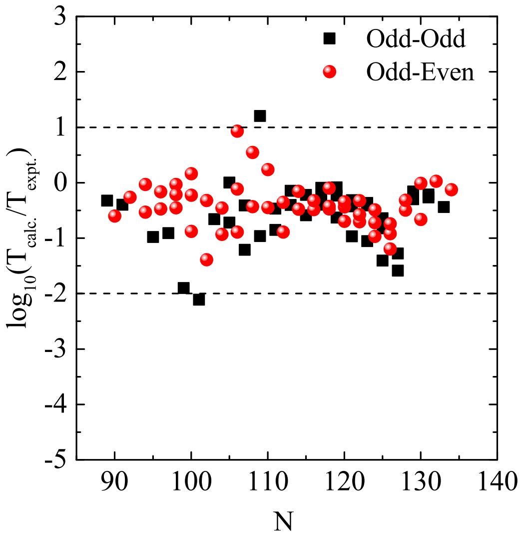

FIG. 7. Deviation of the calculated partial half-lives with the corresponding experimental data for both odd-odd and odd-A nuclei.

constant preformation factor cannot completely describe the detailed features of nuclear structure, one can notice, for some decays, that there is slight deviation with the corresponding experimental data, especially in case of odd-odd nuclei.

Finally, to show the effective strength of our calculations, we have evaluated the standard deviation (σ) of both odd-even and odd-odd half-lives from the expression

$$\sigma = \sqrt{\frac{1}{n-1}\sum_{i=1}^{n}\left[\log_{10}\left(\frac{T_{1/2}^{\text{calc}}}{T_{1/2}^{\text{expt}}}\right)\right]^2} \quad (14)$$

The obtained standard deviation of half-life for odd-even nuclei is 0.580 and that for odd-odd nuclei is 0.830.

IV. SUMMARY AND CONCLUSION

A study of the α-particle preformation probability in the ground state to ground state unfavored decays of odd-even and odd-odd nuclei has been performed. The calculations cover the isotopic chains from Ir to Ac in the mass regions $166 \leqslant A \leqslant 215$ and $77 \leqslant Z \leqslant 89$. We have treated α decay as a one-dimensional problem and worked in the framework of the well-known WKB semiclassical approximation in combination with the Bohr-Sommerfeld quantization condition. The potential barrier is numerically constructed in the well-established double-folding model for both Coulomb and nuclear potentials. A realistic density-dependent CDM3Y1-Paris NN interaction with a finite range exchange part has been used.

Based on the similarity in the behavior of S_α with the neutron number variation for two adjacent elements, we correlate the proton and neutron energy level sequences for the two elements. In this regard, we consider the confirmed nuclear spin and parity assignments of isotopes of an element and predict the unknown or doubted nuclear spin values for other isotopes based on the equality in values or similarity in the behavior of S_α for the isotopes of an element or isotopes of adjacent element. We used two spin coupling rules, namely, the strong and weak rules, to get the values of nuclear spin for odd-odd isotopes. Weak coupling rule has been used for three or four cases only. We used, in some cases, a simple measure for proton-neutron interaction to interpret the behavior of S_α with the neutron number variation. We found that the addition of one proton to the isotopes of Ra with neutron numbers in the range $118 \leqslant N \leqslant 126$ does not affect the behavior of S_α. Moreover, the addition of one neutron to the odd-odd isotopes of Bi keeps the behavior of S_α with the neutron variation almost unchanged.

This study presents a significant step forward in interpreting the rules governing the nuclear spin for odd-odd nuclei based on the behavior of α-particle preformation probability.

[1] D. Ni and Z. Ren, Ann. Phys. (NY) **358**, 108 (2015).
[2] M. Ismail, W. M. Seif, A. Y. Ellithi, and A. Abdurrahman, Phys. Rev. C **92**, 014311 (2015).
[3] W. M. Seif, M. M. Botros, and A. I. Refaie, Phys. Rev. C **92**, 044302 (2015).
[4] D. Bucurescu and N. V. Zamfir, Phys. Rev. C **87**, 054324 (2013).
[5] M. Ismail, A. Y. Ellithi, M. M. Botros, and A. Adel, Phys. Rev. C **81**, 024602 (2010).
[6] Y. Qian, Z. Ren, and D. Ni, Phys. Rev. C **89**, 024318 (2014).
[7] D. Ni, Z. Ren, T. Dong, and Y. Qian, Phys. Rev. C **87**, 024310 (2013).
[8] W. M. Seif, Phys. Rev. C **74**, 034302 (2006).
[9] M. Ismail and A. Adel, Phys. Rev. C **88**, 054604 (2013).
[10] A. Adel and T. Alharbi, Phys. Rev. C **92**, 014619 (2015).
[11] D. Ni and Z. Ren, Phys. Rev. C **87**, 027602 (2013).
[12] Y. T. Oganessian, F. S. Abdullin, and C. Alexander, J. Binder, R. A. Boll, S. N. Dmitriev, J. Ezold, K. Felker, J. M. Gostic, R. K. Grzywacz, J. H. Hamilton, R. A. Henderson, M. G. Itkis, K. Miernik, D. Miller, K. J. Moody, A. N. Polyakov, A. V. Ramayya, J. B. Roberto, M. A. Ryabinin, K. P. Rykaczewski, R. N. Sagaidak, D. A. Shaughnessy, I. V. Shirokovsky, M. V. Shumeiko, M. A. Stoyer, N. J. Stoyer, V. G. Subbotin, A. M. Sukhov, Y. S. Tsyganov, V. K. Utyonkov, A. A. Voinov, and G. K. Vostokin, Phys. Rev. C **87**, 054621 (2013).
[13] Y. T. Oganessian, F. S. Abdullin, S. N. Dmitriev, J. M. Gostic, J. H. Hamilton, R. A. Henderson, M. G. Itkis, K. J. Moody, A. N. Polyakov, A. V. Ramayya, J. B. Roberto, K. P. Rykaczewski, R. N. Sagaidak, D. A. Shaughnessy, I. V. Shirokovsky, M. A. Stoyer, N. J. Stoyer, V. G. Subbotin, A. M. Sukhov, Y. S. Tsyganov, V. K. Utyonkov, A. A. Voinov, and G. K. Vostokin, Phys. Rev. C **87**, 014302 (2013).
[14] Y. T. Oganessian, F. S. Abdullin, C. Alexander, J. Binder, R. A. Boll, S. N. Dmitriev, J. Ezold, K. Felker, J. M. Gostic, R. K. Grzywacz, J. H. Hamilton, R. A. Henderson, M. G. Itkis, K. Miernik, D. Miller, K. J. Moody, A. N. Polyakov, A. V. Ramayya, J. B. Roberto, M. A. Ryabinin, K. P. Rykaczewski, R. N. Sagaidak, D. A. Shaughnessy, I. V. Shirokovsky, M. V. Shumeiko, M. A. Stoyer, N. J. Stoyer, V. G. Subbotin, A. M.

Sukhov, Y. S. Tsyganov, V. K. Utyonkov, A. A. Voinov, and G. K. Vostokin, Phys. Rev. Lett. **109**, 162501 (2012).
[15] Niyti, G. Sawhney, M. K. Sharma, and R. K. Gupta, Phys. Rev. C **91**, 054606 (2015).
[16] G. Gamow, Z. Phys. **51**, 204 (1928).
[17] H. F. Zhang and G. Royer, Phys. Rev. C **77**, 054318 (2008).
[18] S. M. S. Ahmed, R. Yahaya, S. Radiman, and M. S. Yasir, J. Phys. G: Nucl. Part. Phys. **40**, 065105 (2013).
[19] W. M. Seif, M. Shalaby, and M. F. Alrakshy, Phys. Rev. C **84**, 064608 (2011).
[20] S. M. S. Ahmed, R. Yahaya, S. Radiman, M. S. Yasir, H. A. Kassim, and M. U. Khandaker, Eur. Phys. J. A **51**, 13 (2015).
[21] S. Guoa, X. Baoa, Y. Gaoa, J. Lia, and H. Zhang, Nucl. Phys. A **934**, 110 (2015).
[22] M. Ismail and A. Adel, Phys. Rev. C **89**, 034617 (2014).
[23] W. M. Seif, J. Phys. G: Nucl. Part. Phys. **40**, 105102 (2013).
[24] M. Ismail and A. Adel, Phys. Rev. C **86**, 014616 (2012).
[25] M. Ismail and A. Adel, Nucl. Phys. A **912**, 18 (2013).
[26] M. Ismail and A. Adel, Phys. Rev. C **90**, 064624 (2014).
[27] W. M. Seif, Phys. Rev. C **91**, 014322 (2015).
[28] K. Varga, R. G. Lovas, and R. J. Liotta, Phys. Rev. Lett. **69**, 37 (1992).
[29] R. G. Lovas, R. J. Liotta, A. Insolia, K. Varga, and D. S. Delion, Phys. Rep. **294**, 265 (1998).
[30] I. Tonozuka and A. Arima, Nucl. Phys. A **323**, 45 (1979).
[31] G. Dodig-Crnkovic, F. A. Janouch, R. J. Liotta, and L. J. Sibanda, Nucl. Phys. A **444**, 419 (1985).
[32] J. C. Pei, F. R. Xu, Z. J. Lin, and E. G. Zhao, Phys. Rev. C **76**, 044326 (2007).
[33] M. Bhattacharya, S. Roy, and G. Gangopadhyaya, Phys. Lett. B **665**, 182 (2008).
[34] Y. Qian and Z. Ren, Scie. China Phys. Mech. Astron. **56**, 1520 (2013).
[35] N. G. Kelkar and H. M. Castaneda, Phys. Rev. C **76**, 064605 (2007).
[36] C. Xu and Z. Ren, Nucl. Phys. A **753**, 174 (2005).
[37] G. R. Satchler and W. G. Love, Phys. Rep. **55**, 183 (1979).
[38] M. Ismail and A. Adel, Phys. Rev. C **84**, 034610 (2011).
[39] B. Sinha, Phys. Rep. **20**, 1 (1975).
[40] X. Campi and A. Bouyssy, Phys. Lett. B **73**, 263 (1978).
[41] D. T. Khoa, G. R. Satchler, and W. von Oertzen, Phys. Rev. C **56**, 954 (1997).
[42] D. T. Khoa, Phys. Rev. C **63**, 034007 (2001).
[43] M. Ismail, F. Salah, and M. M. Osman, Phys. Rev. C **54**, 3308 (1996).
[44] C. J. Gallagher, Jr. and S. A. Moszkowski, Phys. Rev. **111**, 1282 (1958).
[45] R. F. Casten, Phys. Lett. B **152**, 145 (1985).
[46] R. F. Casten, Phys. Rev. Lett. **54**, 1991 (1985).
[47] R. F. Casten, Nucl. Phys. A **443**, 1 (1985).
[48] NuDat2.6, Nuclear Structure and Decay Data. Available from http://www.nndc.bnl.gov/nudat2/
[49] M. Wang, G. Audi, A. H. Wapstra, F. G. Kondev, M. MacCormick, X. Xu, and B. Pfeiffer, Chin. Phys. C **36**, 1603 (2012).
[50] G. Audi, F. G. Kondev, M. Wang, B. Pfeiffer, X. Sun, J. Blachot, and M. MacCormick, Chin. Phys. C **36**, 1157 (2012).
[51] B. Buck, A. C. Merchant, and S. M. Perez, Phys. Rev. C **51**, 559 (1995).
[52] B. Buck, A. C. Merchant, and S. M. Perez, At. Data Nucl. Data Tables **54**, 53 (1993).
[53] D. Ni and Z. Ren, Phys. Rev. C **81**, 024315 (2010).